

Measurement of the Branching Fractions of $\bar{B} \rightarrow D^{**}\ell^{-}\bar{\nu}_{\ell}$ Decays in Events Tagged by a Fully Reconstructed B Meson

B. Aubert,¹ M. Bona,¹ Y. Karyotakis,¹ J. P. Lees,¹ V. Poireau,¹ E. Prencipe,¹ X. Prudent,¹ V. Tisserand,¹ J. Garra Tico,² E. Grauges,² L. Lopez^{ab,3} A. Palano^{ab,3} M. Pappagallo^{ab,3} G. Eigen,⁴ B. Stugu,⁴ L. Sun,⁴ G. S. Abrams,⁵ M. Battaglia,⁵ D. N. Brown,⁵ R. N. Cahn,⁵ R. G. Jacobsen,⁵ L. T. Kerth,⁵ Yu. G. Kolomensky,⁵ G. Lynch,⁵ I. L. Osipenkov,⁵ M. T. Ronan,^{5,*} K. Tackmann,⁵ T. Tanabe,⁵ C. M. Hawkes,⁶ N. Soni,⁶ A. T. Watson,⁶ H. Koch,⁷ T. Schroeder,⁷ D. Walker,⁸ D. J. Asgeirsson,⁹ B. G. Fulsom,⁹ C. Hearty,⁹ T. S. Mattison,⁹ J. A. McKenna,⁹ M. Barrett,¹⁰ A. Khan,¹⁰ V. E. Blinov,¹¹ A. D. Bukin,¹¹ A. R. Buzykaev,¹¹ V. P. Druzhinin,¹¹ V. B. Golubev,¹¹ A. P. Onuchin,¹¹ S. I. Serednyakov,¹¹ Yu. I. Skovpen,¹¹ E. P. Solodov,¹¹ K. Yu. Todyshev,¹¹ M. Bondioli,¹² S. Curry,¹² I. Eschrich,¹² D. Kirkby,¹² A. J. Lankford,¹² P. Lund,¹² M. Mandelkern,¹² E. C. Martin,¹² D. P. Stoker,¹² S. Abachi,¹³ C. Buchanan,¹³ J. W. Gary,¹⁴ F. Liu,¹⁴ O. Long,¹⁴ B. C. Shen,^{14,*} G. M. Vitug,¹⁴ Z. Yasin,¹⁴ L. Zhang,¹⁴ V. Sharma,¹⁵ C. Campagnari,¹⁶ T. M. Hong,¹⁶ D. Kovalskyi,¹⁶ M. A. Mazur,¹⁶ J. D. Richman,¹⁶ T. W. Beck,¹⁷ A. M. Eisner,¹⁷ C. J. Flacco,¹⁷ C. A. Heusch,¹⁷ J. Kroseberg,¹⁷ W. S. Lockman,¹⁷ T. Schalk,¹⁷ B. A. Schumm,¹⁷ A. Seiden,¹⁷ L. Wang,¹⁷ M. G. Wilson,¹⁷ L. O. Winstrom,¹⁷ C. H. Cheng,¹⁸ D. A. Doll,¹⁸ B. Echenard,¹⁸ F. Fang,¹⁸ D. G. Hitlin,¹⁸ I. Narsky,¹⁸ T. Piatenko,¹⁸ F. C. Porter,¹⁸ R. Andreassen,¹⁹ G. Mancinelli,¹⁹ B. T. Meadows,¹⁹ K. Mishra,¹⁹ M. D. Sokoloff,¹⁹ P. C. Bloom,²⁰ W. T. Ford,²⁰ A. Gaz,²⁰ J. F. Hirschauer,²⁰ M. Nagel,²⁰ U. Nauenberg,²⁰ J. G. Smith,²⁰ K. A. Ulmer,²⁰ S. R. Wagner,²⁰ R. Ayad,^{21,†} A. Soffer,^{21,‡} W. H. Toki,²¹ R. J. Wilson,²¹ D. D. Altenburg,²² E. Feltresi,²² A. Hauke,²² H. Jasper,²² M. Karbach,²² J. Merkel,²² A. Petzold,²² B. Spaan,²² K. Wacker,²² M. J. Kobel,²³ W. F. Mader,²³ R. Nogowski,²³ K. R. Schubert,²³ R. Schwierz,²³ J. E. Sundermann,²³ A. Volk,²³ D. Bernard,²⁴ G. R. Bonneaud,²⁴ E. Latour,²⁴ Ch. Thiebaux,²⁴ M. Verderi,²⁴ P. J. Clark,²⁵ W. Gradl,²⁵ S. Playfer,²⁵ J. E. Watson,²⁵ M. Andreotti^{ab,26} D. Bettoni^{a,26} C. Bozzi^{a,26} R. Calabrese^{ab,26} A. Cecchi^{ab,26} G. Cibinetto^{ab,26} P. Franchini^{ab,26} E. Luppi^{ab,26} M. Negrini^{ab,26} A. Petrella^{ab,26} L. Piemontese^{a,26} V. Santoro^{ab,26} R. Baldini-Ferrolì,²⁷ A. Calcaterra,²⁷ R. de Sangro,²⁷ G. Finocchiaro,²⁷ S. Pacetti,²⁷ P. Patteri,²⁷ I. M. Peruzzi,^{27,§} M. Piccolo,²⁷ M. Rama,²⁷ A. Zallo,²⁷ A. Buzzo^{a,28} R. Contri^{ab,28} M. Lo Vetere^{ab,28} M. M. Macri^{a,28} M. R. Monge^{ab,28} S. Passaggio^{a,28} C. Patrignani^{ab,28} E. Robutti^{a,28} A. Santroni^{ab,28} S. Tosi^{ab,28} K. S. Chaisanguanthum,²⁹ M. Morii,²⁹ J. Marks,³⁰ S. Schenk,³⁰ U. Uwer,³⁰ V. Klose,³¹ H. M. Lacker,³¹ D. J. Bard,³² P. D. Dauncey,³² J. A. Nash,³² W. Panduro Vazquez,³² M. Tibbetts,³² P. K. Behera,³³ X. Chai,³³ M. J. Charles,³³ U. Mallik,³³ J. Cochran,³⁴ H. B. Crawley,³⁴ L. Dong,³⁴ W. T. Meyer,³⁴ S. Prell,³⁴ E. I. Rosenberg,³⁴ A. E. Rubin,³⁴ Y. Y. Gao,³⁵ A. V. Gritsan,³⁵ Z. J. Guo,³⁵ C. K. Lae,³⁵ A. G. Denig,³⁶ M. Fritsch,³⁶ G. Schott,³⁶ N. Arnaud,³⁷ J. Béquilleux,³⁷ A. D'Orazio,³⁷ M. Davier,³⁷ J. Firmino da Costa,³⁷ G. Grosdidier,³⁷ A. Höcker,³⁷ V. Lepeltier,³⁷ F. Le Diberder,³⁷ A. M. Lutz,³⁷ S. Pruvot,³⁷ P. Roudeau,³⁷ M. H. Schune,³⁷ J. Serrano,³⁷ V. Sordini,^{37,¶} A. Stocchi,³⁷ G. Wormser,³⁷ D. J. Lange,³⁸ D. M. Wright,³⁸ I. Bingham,³⁹ J. P. Burke,³⁹ C. A. Chavez,³⁹ J. R. Fry,³⁹ E. Gabathuler,³⁹ R. Gamet,³⁹ D. E. Hutchcroft,³⁹ D. J. Payne,³⁹ C. Touramanis,³⁹ A. J. Bevan,⁴⁰ C. K. Clarke,⁴⁰ K. A. George,⁴⁰ F. Di Lodovico,⁴⁰ R. Sacco,⁴⁰ M. Sigamani,⁴⁰ G. Cowan,⁴¹ H. U. Flaecher,⁴¹ D. A. Hopkins,⁴¹ S. Paramesvaran,⁴¹ F. Salvatore,⁴¹ A. C. Wren,⁴¹ D. N. Brown,⁴² C. L. Davis,⁴² K. E. Alwyn,⁴³ D. Bailey,⁴³ R. J. Barlow,⁴³ Y. M. Chia,⁴³ C. L. Edgar,⁴³ G. Jackson,⁴³ G. D. Lafferty,⁴³ T. J. West,⁴³ J. I. Yi,⁴³ J. Anderson,⁴⁴ C. Chen,⁴⁴ A. Jawahery,⁴⁴ D. A. Roberts,⁴⁴ G. Simi,⁴⁴ J. M. Tuggle,⁴⁴ C. Dallapiccola,⁴⁵ X. Li,⁴⁵ E. Salvati,⁴⁵ S. Saremi,⁴⁵ R. Cowan,⁴⁶ D. Dujmic,⁴⁶ P. H. Fisher,⁴⁶ K. Koenke,⁴⁶ G. Sciolla,⁴⁶ M. Spitznagel,⁴⁶ F. Taylor,⁴⁶ R. K. Yamamoto,⁴⁶ M. Zhao,⁴⁶ P. M. Patel,⁴⁷ S. H. Robertson,⁴⁷ A. Lazzaro^{ab,48} V. Lombardo^{a,48} F. Palombo^{ab,48} J. M. Bauer,⁴⁹ L. Cremaldi,⁴⁹ V. Eschenburg,⁴⁹ R. Godang,^{49,**} R. Kroeger,⁴⁹ D. A. Sanders,⁴⁹ D. J. Summers,⁴⁹ H. W. Zhao,⁴⁹ M. Simard,⁵⁰ P. Taras,⁵⁰ F. B. Viaud,⁵⁰ H. Nicholson,⁵¹ G. De Nardo^{ab,52} L. Lista^{a,52} D. Monorchio^{ab,52} G. Onorato^{ab,52} C. Sciacca^{ab,52} G. Raven,⁵³ H. L. Snoek,⁵³ C. P. Jessop,⁵⁴ K. J. Knoepfel,⁵⁴ J. M. LoSecco,⁵⁴ W. F. Wang,⁵⁴ G. Benelli,⁵⁵ L. A. Corwin,⁵⁵ K. Honscheid,⁵⁵ H. Kagan,⁵⁵ R. Kass,⁵⁵ J. P. Morris,⁵⁵ A. M. Rahimi,⁵⁵ J. J. Regensburger,⁵⁵ S. J. Sekula,⁵⁵ Q. K. Wong,⁵⁵ N. L. Blount,⁵⁶ J. Brau,⁵⁶ R. Frey,⁵⁶ O. Igonkina,⁵⁶ J. A. Kolb,⁵⁶ M. Lu,⁵⁶ R. Rahmat,⁵⁶ N. B. Sinev,⁵⁶ D. Strom,⁵⁶ J. Strube,⁵⁶ E. Torrence,⁵⁶ G. Castelli^{ab,57} N. Gagliardi^{ab,57} M. Margoni^{ab,57} M. Morandin^{a,57} M. Posocco^{a,57} M. Rotondo^{a,57} F. Simonetto^{ab,57} R. Stroili^{ab,57} C. Voci^{ab,57} P. del Amo Sanchez,⁵⁸ E. Ben-Haim,⁵⁸ H. Briand,⁵⁸ G. Calderini,⁵⁸ J. Chauveau,⁵⁸ P. David,⁵⁸ L. Del Buono,⁵⁸ O. Hamon,⁵⁸ Ph. Leruste,⁵⁸ J. Ocariz,⁵⁸ A. Perez,⁵⁸ J. Prendki,⁵⁸ S. Sitt,⁵⁸ L. Gladney,⁵⁹

M. Biasini^{ab,60} R. Covarelli^{ab,60} E. Manoni^{ab,60} C. Angelini^{ab,61} G. Batignani^{ab,61} S. Bettarini^{ab,61}
M. Carpinelli^{ab,61,††} A. Cervelli^{ab,61} F. Forti^{ab,61} M. A. Giorgi^{ab,61} A. Lusiani^{ac,61} G. Marchiori^{ab,61}
M. Morganti^{ab,61} N. Neri^{ab,61} E. Paoloni^{ab,61} G. Rizzo^{ab,61} J. J. Walsh^{a,61} D. Lopes Pegna^{,62} C. Lu^{,62} J. Olsen^{,62}
A. J. S. Smith^{,62} A. V. Telnov^{,62} F. Anulli^{a,63} E. Baracchini^{ab,63} G. Cavoto^{a,63} D. del Re^{ab,63} E. Di Marco^{ab,63}
R. Faccini^{ab,63} F. Ferrarotto^{a,63} F. Ferroni^{ab,63} M. Gaspero^{ab,63} P. D. Jackson^{a,63} L. Li Gioi^{a,63} M. A. Mazzoni^{a,63}
S. Morganti^{a,63} G. Piredda^{a,63} F. Polci^{ab,63} F. Renga^{ab,63} C. Voena^{a,63} M. Ebert^{,64} T. Hartmann^{,64} H. Schröder^{,64}
R. Waldi^{,64} T. Adye^{,65} B. Franek^{,65} E. O. Olaiya^{,65} F. F. Wilson^{,65} S. Emery^{,66} M. Escalier^{,66} L. Esteve^{,66}
S. F. Ganzhur^{,66} G. Hamel de Monchenault^{,66} W. Kozanecki^{,66} G. Vasseur^{,66} Ch. Yèche^{,66} M. Zito^{,66} X. R. Chen^{,67}
H. Liu^{,67} W. Park^{,67} M. V. Purohit^{,67} R. M. White^{,67} J. R. Wilson^{,67} M. T. Allen^{,68} D. Aston^{,68} R. Bartoldus^{,68}
P. Bechtel^{,68} J. F. Benitez^{,68} R. Cenci^{,68} J. P. Coleman^{,68} M. R. Convery^{,68} J. C. Dingfelder^{,68} J. Dorfan^{,68}
G. P. Dubois-Felsmann^{,68} W. Dunwoodie^{,68} R. C. Field^{,68} A. M. Gabareen^{,68} S. J. Gowdy^{,68} M. T. Graham^{,68}
P. Grenier^{,68} C. Hast^{,68} W. R. Innes^{,68} J. Kaminski^{,68} M. H. Kelsey^{,68} H. Kim^{,68} P. Kim^{,68} M. L. Kocian^{,68}
D. W. G. S. Leith^{,68} S. Li^{,68} B. Lindquist^{,68} S. Luitz^{,68} V. Luth^{,68} H. L. Lynch^{,68} D. B. MacFarlane^{,68}
H. Marsiske^{,68} R. Messner^{,68} D. R. Muller^{,68} H. Neal^{,68} S. Nelson^{,68} C. P. O'Grady^{,68} I. Ofte^{,68} A. Perazzo^{,68}
M. Perl^{,68} B. N. Ratcliff^{,68} A. Roodman^{,68} A. A. Salnikov^{,68} R. H. Schindler^{,68} J. Schwiening^{,68} A. Snyder^{,68}
D. Su^{,68} M. K. Sullivan^{,68} K. Suzuki^{,68} S. K. Swain^{,68} J. M. Thompson^{,68} J. Va'vra^{,68} A. P. Wagner^{,68}
M. Weaver^{,68} C. A. West^{,68} W. J. Wisniewski^{,68} M. Wittgen^{,68} D. H. Wright^{,68} H. W. Wulsin^{,68} A. K. Yarritu^{,68}
K. Yi^{,68} C. C. Young^{,68} V. Ziegler^{,68} P. R. Burchat^{,69} A. J. Edwards^{,69} S. A. Majewski^{,69} T. S. Miyashita^{,69}
B. A. Petersen^{,69} L. Wilden^{,69} S. Ahmed^{,70} M. S. Alam^{,70} J. A. Ernst^{,70} B. Pan^{,70} M. A. Saeed^{,70} S. B. Zain^{,70}
S. M. Spanier^{,71} B. J. Wogslund^{,71} R. Eckmann^{,72} J. L. Ritchie^{,72} A. M. Ruland^{,72} C. J. Schilling^{,72}
R. F. Schwitters^{,72} B. W. Drummond^{,73} J. M. Izen^{,73} X. C. Lou^{,73} F. Bianchi^{ab,74} D. Gamba^{ab,74} M. Pelliccioni^{ab,74}
M. Bomben^{ab,75} L. Bosio^{ab,75} C. Cartaro^{ab,75} G. Della Ricca^{ab,75} L. Lanceri^{ab,75} L. Vitale^{ab,75} V. Azzolini^{,76}
N. Lopez-March^{,76} F. Martinez-Vidal^{,76} D. A. Milanes^{,76} A. Oyanguren^{,76} J. Albert^{,77} Sw. Banerjee^{,77}
B. Bhuyan^{,77} H. H. F. Choi^{,77} K. Hamano^{,77} R. Kowalewski^{,77} M. J. Lewczuk^{,77} I. M. Nugent^{,77} J. M. Roney^{,77}
R. J. Sobie^{,77} T. J. Gershon^{,78} P. F. Harrison^{,78} J. Ilic^{,78} T. E. Latham^{,78} G. B. Mohanty^{,78} H. R. Band^{,79}
X. Chen^{,79} S. Dasu^{,79} K. T. Flood^{,79} Y. Pan^{,79} M. Pierini^{,79} R. Prepost^{,79} C. O. Vuosalo^{,79} and S. L. Wu⁷⁹

(The BABAR Collaboration)

¹Laboratoire de Physique des Particules, IN2P3/CNRS et Université de Savoie, F-74941 Annecy-Le-Vieux, France

²Universitat de Barcelona, Facultat de Física, Departament ECM, E-08028 Barcelona, Spain

³INFN Sezione di Bari^a; Dipartimento di Fisica, Università di Bari^b, I-70126 Bari, Italy

⁴University of Bergen, Institute of Physics, N-5007 Bergen, Norway

⁵Lawrence Berkeley National Laboratory and University of California, Berkeley, California 94720, USA

⁶University of Birmingham, Birmingham, B15 2TT, United Kingdom

⁷Ruhr Universität Bochum, Institut für Experimentalphysik 1, D-44780 Bochum, Germany

⁸University of Bristol, Bristol BS8 1TL, United Kingdom

⁹University of British Columbia, Vancouver, British Columbia, Canada V6T 1Z1

¹⁰Brunel University, Uxbridge, Middlesex UB8 3PH, United Kingdom

¹¹Budker Institute of Nuclear Physics, Novosibirsk 630090, Russia

¹²University of California at Irvine, Irvine, California 92697, USA

¹³University of California at Los Angeles, Los Angeles, California 90024, USA

¹⁴University of California at Riverside, Riverside, California 92521, USA

¹⁵University of California at San Diego, La Jolla, California 92093, USA

¹⁶University of California at Santa Barbara, Santa Barbara, California 93106, USA

¹⁷University of California at Santa Cruz, Institute for Particle Physics, Santa Cruz, California 95064, USA

¹⁸California Institute of Technology, Pasadena, California 91125, USA

¹⁹University of Cincinnati, Cincinnati, Ohio 45221, USA

²⁰University of Colorado, Boulder, Colorado 80309, USA

²¹Colorado State University, Fort Collins, Colorado 80523, USA

²²Technische Universität Dortmund, Fakultät Physik, D-44221 Dortmund, Germany

²³Technische Universität Dresden, Institut für Kern- und Teilchenphysik, D-01062 Dresden, Germany

²⁴Laboratoire Leprince-Ringuet, CNRS/IN2P3, Ecole Polytechnique, F-91128 Palaiseau, France

²⁵University of Edinburgh, Edinburgh EH9 3JZ, United Kingdom

²⁶INFN Sezione di Ferrara^a; Dipartimento di Fisica, Università di Ferrara^b, I-44100 Ferrara, Italy

²⁷INFN Laboratori Nazionali di Frascati, I-00044 Frascati, Italy

²⁸INFN Sezione di Genova^a; Dipartimento di Fisica, Università di Genova^b, I-16146 Genova, Italy

²⁹Harvard University, Cambridge, Massachusetts 02138, USA

³⁰Universität Heidelberg, Physikalisches Institut, Philosophenweg 12, D-69120 Heidelberg, Germany

- ³¹Humboldt-Universität zu Berlin, Institut für Physik, Newtonstr. 15, D-12489 Berlin, Germany
- ³²Imperial College London, London, SW7 2AZ, United Kingdom
- ³³University of Iowa, Iowa City, Iowa 52242, USA
- ³⁴Iowa State University, Ames, Iowa 50011-3160, USA
- ³⁵Johns Hopkins University, Baltimore, Maryland 21218, USA
- ³⁶Universität Karlsruhe, Institut für Experimentelle Kernphysik, D-76021 Karlsruhe, Germany
- ³⁷Laboratoire de l'Accélérateur Linéaire, IN2P3/CNRS et Université Paris-Sud 11, Centre Scientifique d'Orsay, B. P. 34, F-91898 Orsay Cedex, France
- ³⁸Lawrence Livermore National Laboratory, Livermore, California 94550, USA
- ³⁹University of Liverpool, Liverpool L69 7ZE, United Kingdom
- ⁴⁰Queen Mary, University of London, London, E1 4NS, United Kingdom
- ⁴¹University of London, Royal Holloway and Bedford New College, Egham, Surrey TW20 0EX, United Kingdom
- ⁴²University of Louisville, Louisville, Kentucky 40292, USA
- ⁴³University of Manchester, Manchester M13 9PL, United Kingdom
- ⁴⁴University of Maryland, College Park, Maryland 20742, USA
- ⁴⁵University of Massachusetts, Amherst, Massachusetts 01003, USA
- ⁴⁶Massachusetts Institute of Technology, Laboratory for Nuclear Science, Cambridge, Massachusetts 02139, USA
- ⁴⁷McGill University, Montréal, Québec, Canada H3A 2T8
- ⁴⁸INFN Sezione di Milano^a; Dipartimento di Fisica, Università di Milano^b, I-20133 Milano, Italy
- ⁴⁹University of Mississippi, University, Mississippi 38677, USA
- ⁵⁰Université de Montréal, Physique des Particules, Montréal, Québec, Canada H3C 3J7
- ⁵¹Mount Holyoke College, South Hadley, Massachusetts 01075, USA
- ⁵²INFN Sezione di Napoli^a; Dipartimento di Scienze Fisiche, Università di Napoli Federico II^b, I-80126 Napoli, Italy
- ⁵³NIKHEF, National Institute for Nuclear Physics and High Energy Physics, NL-1009 DB Amsterdam, The Netherlands
- ⁵⁴University of Notre Dame, Notre Dame, Indiana 46556, USA
- ⁵⁵Ohio State University, Columbus, Ohio 43210, USA
- ⁵⁶University of Oregon, Eugene, Oregon 97403, USA
- ⁵⁷INFN Sezione di Padova^a; Dipartimento di Fisica, Università di Padova^b, I-35131 Padova, Italy
- ⁵⁸Laboratoire de Physique Nucléaire et de Hautes Energies, IN2P3/CNRS, Université Pierre et Marie Curie-Paris6, Université Denis Diderot-Paris7, F-75252 Paris, France
- ⁵⁹University of Pennsylvania, Philadelphia, Pennsylvania 19104, USA
- ⁶⁰INFN Sezione di Perugia^a; Dipartimento di Fisica, Università di Perugia^b, I-06100 Perugia, Italy
- ⁶¹INFN Sezione di Pisa^a; Dipartimento di Fisica, Università di Pisa^b; Scuola Normale Superiore di Pisa^c, I-56127 Pisa, Italy
- ⁶²Princeton University, Princeton, New Jersey 08544, USA
- ⁶³INFN Sezione di Roma^a; Dipartimento di Fisica, Università di Roma La Sapienza^b, I-00185 Roma, Italy
- ⁶⁴Universität Rostock, D-18051 Rostock, Germany
- ⁶⁵Rutherford Appleton Laboratory, Chilton, Didcot, Oxon, OX11 0QX, United Kingdom
- ⁶⁶DSM/Irfu, CEA/Saclay, F-91191 Gif-sur-Yvette Cedex, France
- ⁶⁷University of South Carolina, Columbia, South Carolina 29208, USA
- ⁶⁸Stanford Linear Accelerator Center, Stanford, California 94309, USA
- ⁶⁹Stanford University, Stanford, California 94305-4060, USA
- ⁷⁰State University of New York, Albany, New York 12222, USA
- ⁷¹University of Tennessee, Knoxville, Tennessee 37996, USA
- ⁷²University of Texas at Austin, Austin, Texas 78712, USA
- ⁷³University of Texas at Dallas, Richardson, Texas 75083, USA
- ⁷⁴INFN Sezione di Torino^a; Dipartimento di Fisica Sperimentale, Università di Torino^b, I-10125 Torino, Italy
- ⁷⁵INFN Sezione di Trieste^a; Dipartimento di Fisica, Università di Trieste^b, I-34127 Trieste, Italy
- ⁷⁶IFIC, Universitat de Valencia-CSIC, E-46071 Valencia, Spain
- ⁷⁷University of Victoria, Victoria, British Columbia, Canada V8W 3P6
- ⁷⁸Department of Physics, University of Warwick, Coventry CV4 7AL, United Kingdom
- ⁷⁹University of Wisconsin, Madison, Wisconsin 53706, USA
- (Dated: August 4, 2008)

We report a measurement of the branching fractions of $\bar{B} \rightarrow D^{**}\ell^{-}\bar{\nu}_{\ell}$ decays based on 417 fb^{-1} of data collected at the $\Upsilon(4S)$ resonance with the BABAR detector at the PEP-II $e^{+}e^{-}$ storage rings. Events are selected by fully reconstructing one of the B mesons in a hadronic decay mode. A fit to the invariant mass differences $m(D^{(*)}\pi) - m(D^{(*)})$ is performed to extract the signal yields of the different D^{**} states. We observe the $\bar{B} \rightarrow D^{**}\ell^{-}\bar{\nu}_{\ell}$ decay modes corresponding to the four D^{**} states predicted by Heavy Quark Symmetry with a significance greater than six standard deviations including systematic uncertainties.

Semileptonic B decays to orbitally-excited P-wave charm mesons (D^{**}) are of interest for several reasons. Improved knowledge of the branching fractions for these decays is important to reduce the systematic uncertainty in the measurements of the Cabibbo-Kobayashi-Maskawa [1] matrix elements $|V_{cb}|$ and $|V_{ub}|$. For example, one of the leading sources of systematic uncertainty on $|V_{cb}|$ measurements from $\bar{B} \rightarrow D^* \ell^- \bar{\nu}_\ell$ decays [2] is the limited knowledge of the background due to $\bar{B} \rightarrow D^{**} \ell^- \bar{\nu}_\ell$ [3].

The D^{**} mesons contain one charm quark and one light quark with relative angular momentum $L = 1$. According to Heavy Quark Symmetry (HQS) [4], they form one doublet of states with angular momentum $j \equiv s_q + L = 3/2$ [$D_1(2420), D_2^*(2460)$] and another doublet with $j = 1/2$ [$D_0^*(2400), D_1'(2430)$], where s_q is the light quark spin. Parity and angular momentum conservation constrain the decays allowed for each state. The D_1 and D_2^* states decay through a D-wave to $D^* \pi$ and $D^{(*)} \pi$, respectively, and have small decay widths, while the D_0^* and D_1' states decay through an S-wave to $D \pi$ and $D^* \pi$ and are very broad.

$\bar{B} \rightarrow D^{**} \ell^- \bar{\nu}_\ell$ decays constitute a significant fraction of B semileptonic decays [5] and may help to explain the discrepancy between the inclusive $\bar{B} \rightarrow X \ell^- \bar{\nu}_\ell$ rate and the sum of the measured exclusive decay rates [5, 6, 7]. The measured decay properties for $\bar{B} \rightarrow D^{**} \ell^- \bar{\nu}_\ell$ can be compared with the predictions of the Heavy Quark Effective Theory (HQET) [8]. QCD sum rules [9] imply the strong dominance of B decays to the narrow D^{**} states over those to the wide ones, while some experimental data show the opposite trend [10, 11].

In this letter, we present the observation of B semileptonic decays into the four excited D mesons predicted by HQS and measure the $\mathcal{B}(\bar{B} \rightarrow D^{**} \ell^- \bar{\nu}_\ell)$ branching fractions. The analysis is based on data collected with the BABAR detector [12] at the PEP-II asymmetric-energy e^+e^- storage rings at SLAC. The data consist of a total of 417 fb^{-1} recorded at the $\Upsilon(4S)$ resonance, corresponding to approximately 460 million $B\bar{B}$ pairs. An additional 40 fb^{-1} , taken at a center-of-mass (CM) energy 40 MeV below the $\Upsilon(4S)$ resonance, is used to study background from $e^+e^- \rightarrow f\bar{f}$ ($f = u, d, s, c, \tau$) continuum events. A detailed GEANT4-based Monte Carlo (MC) simulation [13] of $B\bar{B}$ and continuum events is used to study the detector response, its acceptance, and to validate the analysis techniques. The simulation describes $\bar{B} \rightarrow D^{**} \ell^- \bar{\nu}_\ell$ decays using the ISGW2 model [14], and non-resonant $\bar{B} \rightarrow D^{(*)} \pi \ell^- \bar{\nu}_\ell$ decays using the model of Goity and Roberts [15].

We select semileptonic $\bar{B} \rightarrow D^{**} \ell^- \bar{\nu}_\ell$ decays with $\ell = e, \mu$ in events containing a fully reconstructed B meson (B_{tag}), which allows us to constrain the kinematics,

reduce the combinatorial background, and determine the charge and flavor of the signal B meson. D^{**} mesons are reconstructed in the $D^{(*)} \pi^\pm$ decay modes and the different D^{**} states are identified by a fit to the invariant mass differences $m(D^{(*)} \pi) - m(D^{(*)})$.

We first reconstruct the semileptonic B decay, selecting a lepton with momentum p_ℓ^* in the CM frame larger than $0.6 \text{ GeV}/c$. We search for pairs of oppositely-charged tracks that form a vertex and remove those with an invariant mass consistent with a photon conversion or a π^0 Dalitz decay. Candidate D^0 mesons that have the correct charge correlation with the lepton are reconstructed in the $K^- \pi^+$, $K^- \pi^+ \pi^0$, $K^- \pi^+ \pi^+ \pi^-$, $K_S^0 \pi^+ \pi^-$, $K_S^0 \pi^+ \pi^- \pi^0$, $K_S^0 \pi^0$, $K^+ K^-$, $\pi^+ \pi^-$, and $K_S^0 K_S^0$ channels, and D^+ mesons in the $K^- \pi^+ \pi^+$, $K^- \pi^+ \pi^+ \pi^0$, $K_S^0 \pi^+$, $K_S^0 \pi^+ \pi^0$, $K^+ K^- \pi^+$, $K_S^0 K^+$, and $K_S^0 \pi^+ \pi^+ \pi^-$ channels. In events with multiple $D \ell^-$ combinations, the candidate with the best D - ℓ vertex fit is selected. Candidate D^* mesons are reconstructed by combining a D candidate with a pion or a photon in the $D^{*+} \rightarrow D^0 \pi^+$, $D^{*+} \rightarrow D^+ \pi^0$, $D^{*0} \rightarrow D^0 \pi^0$, and $D^{*0} \rightarrow D^0 \gamma$ channels. In events with multiple $D^* \ell^-$ combinations, we choose the candidate with the smallest χ^2 based on the deviations from the nominal values of the D invariant mass and the invariant mass difference between the D^* and the D , using the resolution measured in each mode.

We reconstruct B_{tag} decays [16] in charmed hadronic modes $\bar{B} \rightarrow DY$, where Y represents a collection of hadrons, composed of $n_1 \pi^\pm + n_2 K^\pm + n_3 K_S^0 + n_4 \pi^0$, where $n_1 + n_2 = 1, 3, 5$, $n_3 \leq 2$, and $n_4 \leq 2$. Using $D^0(D^+)$ and $D^{*0}(D^{*+})$ as seeds for $B^-(\bar{B}^0)$ decays, we reconstruct about 1000 different decay chains.

The kinematic consistency of a B_{tag} candidate with a B meson decay is evaluated using two variables: the beam-energy substituted mass $m_{ES} \equiv \sqrt{s/4 - |p_B^*|^2}$, and the energy difference $\Delta E \equiv E_B^* - \sqrt{s}/2$. Here \sqrt{s} is the total CM energy, and p_B^* and E_B^* denote the momentum and energy of the B_{tag} candidate in the CM frame. For correctly identified B_{tag} decays, the m_{ES} distribution peaks at the B meson mass, while ΔE is consistent with zero. We select B_{tag} candidates in the signal region defined as $5.27 \text{ GeV}/c^2 < m_{ES} < 5.29 \text{ GeV}/c^2$, excluding those with daughter particles in common with the charm meson or the lepton from the semileptonic B decay. In the case of multiple B_{tag} candidates in an event, we select the one with the smallest $|\Delta E|$ value. The B_{tag} and the $D^{(*)} \ell$ candidates are required to have the correct charge-flavor correlation. We account for mixing effects in the \bar{B}^0 sample as described in Ref. [17]. Cross-feed effects, *i.e.*, $B_{\text{tag}}^-(\bar{B}_{\text{tag}}^0)$ candidates erroneously reconstructed as a neutral (charged) B , are subtracted using estimates from the simulation.

We reconstruct $B^- \rightarrow D^{(*)+} \pi^- \ell^- \bar{\nu}_\ell$ and $\bar{B}^0 \rightarrow$

TABLE I: m_{miss}^2 selection criteria.

Mode	Selection Criteria
$B^- \rightarrow D^{*+}\pi^-\ell^-\bar{\nu}_\ell$	$-0.25 < m_{\text{miss}}^2 < 0.25 \text{ GeV}^2/c^4$
$B^- \rightarrow D^+\pi^-\ell^-\bar{\nu}_\ell$	$-0.25 < m_{\text{miss}}^2 < 0.8 \text{ GeV}^2/c^4$
$\bar{B}^0 \rightarrow D^{*0}\pi^+\ell^-\bar{\nu}_\ell$	$-0.2 < m_{\text{miss}}^2 < 0.35 \text{ GeV}^2/c^4$
$\bar{B}^0 \rightarrow D^0\pi^+\ell^-\bar{\nu}_\ell$	$-0.15 < m_{\text{miss}}^2 < 0.85 \text{ GeV}^2/c^4$

$D^{(*)0}\pi^+\ell^-\bar{\nu}_\ell$ decays starting from the corresponding $B_{\text{tag}} + D^{(*)}\ell^-$ combinations. We select events with only one additional reconstructed charged track, correctly matched to the $D^{(*)}$ flavor, that has not been used for the reconstruction of the B_{tag} , the signal $D^{(*)}$, or the lepton. $D(D^*)$ candidates are selected within 2σ (1.5-2.5 σ , depending on the D^* decay mode) of the D mass ($D^* - D$ mass difference), where the resolution σ is typically around 8 (1-7) MeV/ c^2 . For the $\bar{B}^0 \rightarrow D^{(*)0}\pi^+\ell^-\bar{\nu}_\ell$ decay, we additionally require the invariant mass difference $m(D^0\pi^+) - m(D^0)$ to be greater than 0.18 GeV/ c^2 to veto $\bar{B}^0 \rightarrow D^{*+}\ell^-\bar{\nu}_\ell$ events.

Semileptonic $\bar{B} \rightarrow D^{*}\ell^-\bar{\nu}_\ell$ decays are identified by the missing mass squared in the event, $m_{\text{miss}}^2 = [p(\Upsilon(4S)) - p(B_{\text{tag}}) - p(D^{(*)}\pi) - p(\ell)]^2$, defined in terms of the particle four-momenta. For correctly reconstructed signal events, the only missing particle is the neutrino, and m_{miss}^2 peaks at zero. Other B semileptonic decays, where one particle is not reconstructed (feed-down) or is erroneously added to the charm candidate (feed-up), exhibit higher or lower values in m_{miss}^2 [7]. In feed-down cases where both a D and a D^* candidate have been reconstructed, we keep only the latter candidate.

The m_{miss}^2 selection criteria are listed in Table I. The m_{miss}^2 region between 0.2 and 1 GeV $^2/c^4$ for $\bar{B} \rightarrow D\pi\ell^-\bar{\nu}_\ell$ events is dominated by feed-down from $\bar{B} \rightarrow D^{*}(\rightarrow D^*\pi)\ell^-\bar{\nu}_\ell$ semileptonic decays where the soft pion from the D^* decay is not reconstructed. In order to retain these events we apply an asymmetric cut on m_{miss}^2 for these modes.

The signal yields for the $\bar{B} \rightarrow D^{*}\ell^-\bar{\nu}_\ell$ decays are extracted through a simultaneous unbinned maximum likelihood fit to the four $m(D^{(*)}\pi) - m(D^{(*)})$ distributions. With the current statistics, validation studies on MC samples show that our sensitivity to non-resonant $\bar{B} \rightarrow D^{(*)}\pi\ell^-\bar{\nu}_\ell$ decays is limited. Including hypotheses for these components results in a fitted contribution that is consistent with zero. Thus we assume that these non-resonant contributions are negligible. The probability that $\bar{B} \rightarrow D^{*}(\rightarrow D^*\pi)\ell^-\bar{\nu}_\ell$ decays are reconstructed as $\bar{B} \rightarrow D^{*}(\rightarrow D\pi)\ell^-\bar{\nu}_\ell$ is determined with the MC simulation to be 26%(59%) for the $B^-(\bar{B}^0)$ sample and held fixed in the fit.

The Probability Density Functions (PDFs) for the D^{*} signal components are determined using MC $\bar{B} \rightarrow D^{*}\ell^-\bar{\nu}_\ell$ signal events. A convolution of a Breit-Wigner

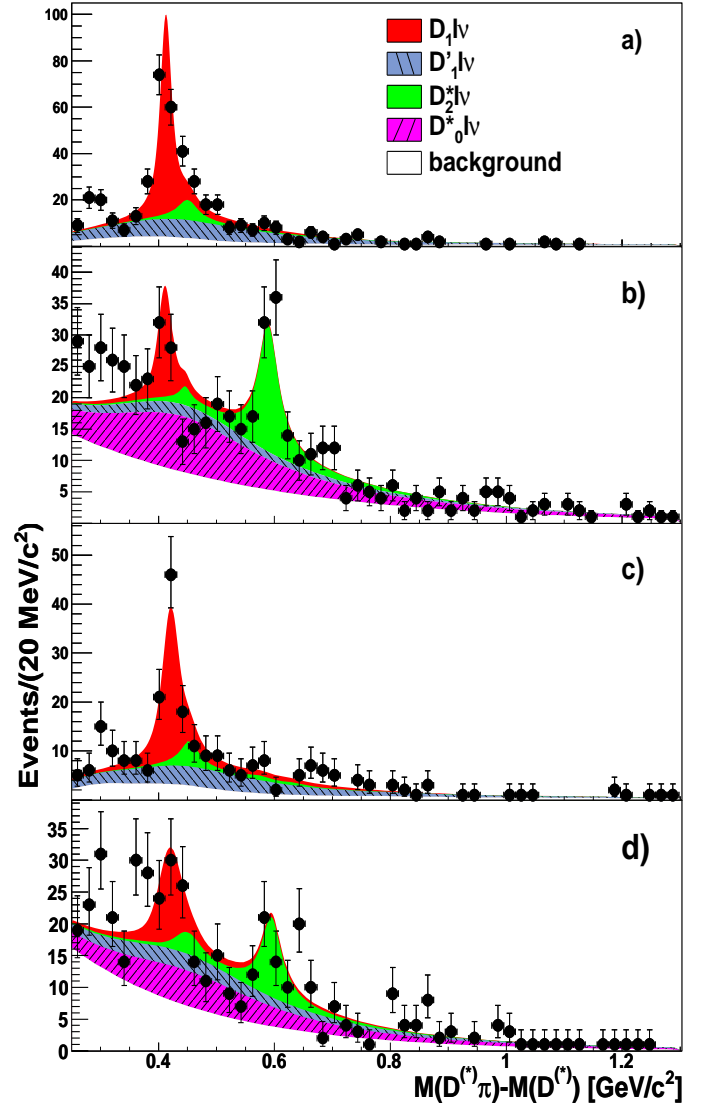


FIG. 1: (Color online) Fit to the $m(D^{(*)}\pi) - m(D^{(*)})$ distribution for a) $B^- \rightarrow D^{*+}\pi^-\ell^-\bar{\nu}_\ell$, b) $B^- \rightarrow D^+\pi^-\ell^-\bar{\nu}_\ell$, c) $\bar{B}^0 \rightarrow D^{*0}\pi^+\ell^-\bar{\nu}_\ell$, and d) $\bar{B}^0 \rightarrow D^0\pi^+\ell^-\bar{\nu}_\ell$: the data (points with error bars) are compared to the results of the overall fit (sum of the solid distributions). The PDFs for the different fit components are stacked and shown in different colors.

function with a Gaussian, whose resolution is determined from the simulation, is used to model the D^{*} resonances. The D^{*} masses and widths are fixed to measured values [5]. We rely on the MC prediction for the shape of the combinatorial and continuum background. A non-parametric KEYS function [18] is used to model this component for the $D^*\pi\ell^-\bar{\nu}_\ell$ sample, while for the $D\pi\ell^-\bar{\nu}_\ell$ sample we use the convolution of an exponential with a Gaussian to model the tail from virtual D^* mesons. The combinatorial and continuum background yields are estimated from data. We fit the hadronic $B_{\text{tag}} m_{ES}$ distributions for $\bar{B} \rightarrow D^{*}\ell^-\bar{\nu}_\ell$ events as described in [7],

and we obtain the number of background events from the integral of the background function in the m_{ES} signal region.

Table II summarizes the results from two fits: one in which we fit the charged and neutral B samples separately, and one in which we impose the isospin constraints $\mathcal{B}(B^- \rightarrow D^{**}\ell^- \bar{\nu}_\ell)/\mathcal{B}(\bar{B}^0 \rightarrow D^{**}\ell^- \bar{\nu}_\ell) = \tau_{B^-}/\tau_{\bar{B}^0}$. The latter fit yields a significance greater than 6 standard deviations for all four D^{**} states including systematic uncertainties. The results of this fit are shown in Fig. 1.

The D_2^* contributes to both the $D\pi$ and the $D^*\pi$ samples. In the nominal fit we fix the ratio $\mathcal{B}(D_2^* \rightarrow D\pi)/\mathcal{B}(D_2^* \rightarrow D^*\pi)$ to 2.2 [5]. When we allow this ratio to float we obtain 1.9 ± 0.6 .

To reduce systematic uncertainties we measure the ratios of the $\mathcal{B}(\bar{B} \rightarrow D^{**}\ell^- \bar{\nu}_\ell)$ branching fractions to the inclusive \bar{B}^0 and B^- semileptonic branching fractions. A sample of $\bar{B} \rightarrow X\ell^- \bar{\nu}_\ell$ events is selected by identifying a charged lepton with $p_\ell^* > 0.6$ GeV/ c and the correct charge correlation with the B_{tag} candidate. In the case of multiple B_{tag} candidates in an event, we select the one reconstructed in the decay channel with the highest purity, defined as the fraction of signal events in the m_{ES} signal region. Background components that peak in the m_{ES} signal region include cascade B meson decays (*i.e.*, the lepton does not come directly from the B) and hadronic decays, and are subtracted using the corresponding MC predictions.

The total yield for the inclusive $\bar{B} \rightarrow X\ell^- \bar{\nu}_\ell$ decays is obtained from a maximum likelihood fit to the m_{ES} distribution of the B_{tag} candidates, as described in [7]. The fit yields $198,897 \pm 1,578$ events for the $B^- \rightarrow X\ell^- \bar{\nu}_\ell$ sample and $120,168 \pm 1,036$ events for the $\bar{B}^0 \rightarrow X\ell^- \bar{\nu}_\ell$ sample.

The ratios $\mathcal{B}(\bar{B} \rightarrow D^{**}\ell^- \bar{\nu}_\ell)/\mathcal{B}(\bar{B} \rightarrow X\ell^- \bar{\nu}_\ell) = (N_{\text{sig}}/\epsilon_{\text{sig}}) \cdot (\epsilon_{\text{sl}}/N_{\text{sl}})$ are obtained by correcting the signal yields for the reconstruction efficiencies (estimated from $B\bar{B}$ MC events). Here, N_{sig} is the number of $\bar{B} \rightarrow D^{**}\ell^- \bar{\nu}_\ell$ signal events, reported in Table II together with the corresponding reconstruction efficiencies ϵ_{sig} , N_{sl} is the $\bar{B} \rightarrow X\ell^- \bar{\nu}_\ell$ signal yield, and ϵ_{sl} is the corresponding reconstruction efficiency including the B_{tag} reconstruction, equal to 0.39% and 0.25% for the $B^- \rightarrow X\ell^- \bar{\nu}_\ell$ and $\bar{B}^0 \rightarrow X\ell^- \bar{\nu}_\ell$ decays, respectively. The absolute branching fractions $\mathcal{B}(\bar{B} \rightarrow D^{**}\ell^- \bar{\nu}_\ell)$ are then determined using the semileptonic branching fraction $\mathcal{B}(\bar{B} \rightarrow X\ell^- \bar{\nu}_\ell) = (10.78 \pm 0.18)\%$ and the ratio of the \bar{B}^0 and the B^- lifetimes $\tau_{B^-}/\tau_{\bar{B}^0} = 1.071 \pm 0.009$ [5].

Numerous sources of systematic uncertainties have been investigated. The largest uncertainty is due to the determination of the $\bar{B} \rightarrow D^{**}\ell^- \bar{\nu}_\ell$ signal yields (resulting in 5.5-17.0% relative systematic uncertainty depending on the D^{**} state). This uncertainty is estimated using ensembles of fits to the data in which the input parameters are varied within the known uncertainties in the PDF parameterization (0.2-8.7%), the shape and yield of the

combinatorial and continuum background (0.2-10.4%), the modeling of the broad D^{**} states (4.5-13.8%), and the D^* feed-down rate (0.5-4.0%). We check that the combinatorial and continuum background shape is well reproduced by the simulation by verifying that the MC samples of right-sign and wrong-sign $D^{(*)}\pi$ combinations have similar shapes, and that the wrong-sign distribution in the data agrees well with that in the simulation. We observe an excess of events in the low invariant mass difference region in the four samples that is not accounted for by the background PDF. We study $\bar{B} \rightarrow D^{(*)}n\pi\ell^- \bar{\nu}_\ell$ ($n > 1$) decays, not included in our standard MC simulation, as a possible source of this excess. We use different MC models for these decays, and find that they do not account for all the observed excess. We evaluate a corresponding systematic uncertainty (0.1-3.2%), included in the yield uncertainty above. The uncertainties due to the detector simulation are determined by varying, within bounds given by data control samples, the charged track reconstruction efficiency (1.3-2.0%), the photon reconstruction efficiency (0.2-4.8%), the lepton identification efficiency (1.2-1.6%), and the reconstruction efficiency for low momentum charged (1.2%) and neutral pions (1.3%). We use an HQET model [8] to test the model dependence of the $\bar{B} \rightarrow D^{**}\ell^- \bar{\nu}_\ell$ simulation (0.8-2.5%). We include the uncertainty on the branching fractions of the reconstructed D and D^* modes (3.0-4.5%), and on the absolute branching fraction $\mathcal{B}(\bar{B} \rightarrow X\ell^- \bar{\nu}_\ell)$ used for the normalization (1.9%). We also include a systematic uncertainty due to differences in the efficiency of the B_{tag} selection in the exclusive selection of $\bar{B} \rightarrow D^{**}\ell^- \bar{\nu}_\ell$ decays and the inclusive $\bar{B} \rightarrow X\ell^- \bar{\nu}_\ell$ reconstruction (4.0-5.6%).

In conclusion, we report the simultaneous observation of $\bar{B} \rightarrow D^{**}\ell^- \bar{\nu}_\ell$ decays into the four D^{**} states predicted by HQS. The measured branching fractions are reported in Table II. We find results consistent with Ref. [7] for the sum of the different D^{**} branching fractions. The rate for the D^{**} narrow states is in good agreement with recent measurements [19]; the one for the broad states is in agreement with DELPHI [11] but does not agree with the D_1' limit of Belle [10]. The rate for the broad states is found to be large. If these broad states are indeed due to $\bar{B} \rightarrow D_1'\ell^- \bar{\nu}_\ell$ and $\bar{B} \rightarrow D_0^*\ell^- \bar{\nu}_\ell$ decays, this is in conflict with the expectations from QCD sum rules.

We are grateful for the excellent luminosity and machine conditions provided by our PEP-II colleagues, and for the substantial dedicated effort from the computing organizations that support BABAR. The collaborating institutions wish to thank SLAC for its support and kind hospitality. This work is supported by DOE and NSF (USA), NSERC (Canada), CEA and CNRS-IN2P3 (France), BMBF and DFG (Germany), INFN (Italy), FOM (The Netherlands), NFR (Norway), MIST (Russia), MEC (Spain), and STFC (United Kingdom). Individuals have received support from the Marie Curie EIF (European Union) and the A. P. Sloan Foundation.

TABLE II: Results from the fits to data: the $\bar{B} \rightarrow D^{**}\ell^- \bar{\nu}_\ell$ signal yield, the corresponding reconstruction efficiency, the product of branching fractions, where the first error is statistical and the second systematic. For the $\bar{B} \rightarrow D_2^* \ell^- \bar{\nu}_\ell$ decay, we report yields and product of branching fractions for the $D_2^* \rightarrow D\pi$ decay mode. For the isospin-constrained results (last two columns), the B^- branching fraction products are reported. The statistical significances, S_{stat} , are obtained by computing the difference in the log likelihood between the nominal fit and the fit in which we fix the different signal components to 0. The significances including the systematic uncertainty, S_{tot} , are obtained by rescaling the statistical significances by $\sigma_{\text{stat}}/\sqrt{\sigma_{\text{stat}}^2 + \sigma_{\text{syst}}^2}$.

Decay Mode	Yield	$\epsilon_{\text{sig}} (\times 10^{-4})$	$\mathcal{B}(\bar{B} \rightarrow D^{**}\ell^-\bar{\nu}_\ell) \times \mathcal{B}(D^{**} \rightarrow D^{(*)}\pi^\pm)$	%	$S_{\text{tot}}(S_{\text{stat}})$	\mathcal{B} %	$S_{\text{tot}}(S_{\text{stat}})$
$B^- \rightarrow D_1^0 \ell^- \bar{\nu}_\ell$	165 ± 18	1.24	$0.29 \pm 0.03 \pm 0.03$	9.9 (12.7)	$0.29 \pm 0.03 \pm 0.03$	10.7 (15.2)	
$B^- \rightarrow D_2^{*0} \ell^- \bar{\nu}_\ell$	97 ± 16	1.44	$0.15 \pm 0.02 \pm 0.01$	6.3 (7.3)	$0.12 \pm 0.02 \pm 0.01$	6.0 (7.4)	
$B^- \rightarrow D_1^{*0} \ell^- \bar{\nu}_\ell$	142 ± 21	1.13	$0.27 \pm 0.04 \pm 0.05$	5.4 (8.0)	$0.30 \pm 0.03 \pm 0.04$	6.4 (10.0)	
$B^- \rightarrow D_0^{*0} \ell^- \bar{\nu}_\ell$	137 ± 26	1.15	$0.26 \pm 0.05 \pm 0.04$	4.5 (5.8)	$0.32 \pm 0.04 \pm 0.04$	6.1 (8.3)	
$\bar{B}^0 \rightarrow D_1^+ \ell^- \bar{\nu}_\ell$	88 ± 14	0.70	$0.27 \pm 0.04 \pm 0.03$	7.0 (8.4)			
$\bar{B}^0 \rightarrow D_2^{*+} \ell^- \bar{\nu}_\ell$	29 ± 13	0.91	$0.07 \pm 0.03 \pm 0.01$ (< 0.11 @90% CL)	2.3 (2.5)			
$\bar{B}^0 \rightarrow D_1^{*+} \ell^- \bar{\nu}_\ell$	86 ± 18	0.60	$0.31 \pm 0.07 \pm 0.05$	4.6 (5.8)			
$\bar{B}^0 \rightarrow D_0^{*+} \ell^- \bar{\nu}_\ell$	142 ± 26	0.70	$0.44 \pm 0.08 \pm 0.06$	4.7 (6.0)			

* Deceased

† Now at Temple University, Philadelphia, Pennsylvania 19122, USA

‡ Now at Tel Aviv University, Tel Aviv, 69978, Israel

§ Also with Università di Perugia, Dipartimento di Fisica, Perugia, Italy

¶ Also with Università di Roma La Sapienza, I-00185 Roma, Italy

** Now at University of South Alabama, Mobile, Alabama 36688, USA

†† Also with Università di Sassari, Sassari, Italy

[1] M. Kobayashi and T. Maskawa, Prog. Theor. Phys. **49**, 652 (1973).

[2] The charge conjugate state is always implied unless stated otherwise.

[3] B. Aubert *et al.* (BABAR Collab.), Phys. Rev. D **77**, 032002 (2008).

[4] N. Isgur and M. B. Wise, Phys. Rev. Lett. **66**, 1130 (1991).

[5] W. -M. Yao *et al.* (Particle Data Group), J. Phys. G **33**, 1 (2006).

[6] B. Aubert *et al.* (BABAR Collab.), Phys. Rev. D **76**, 051101 (2007).

[7] B. Aubert *et al.* (BABAR Collab.), Phys. Rev. Lett. **100**, 151802 (2008).

[8] A. K. Leibovich, Z. Ligeti, I. W. Stewart and M. B. Wise, Phys. Rev. D **57**, 308 (1998).

[9] N. Uraltsev, Phys. Lett. B. **501**, 86 (2001).

[10] D. Liventsev *et al.* (Belle Collab.), Phys. Rev. D **77**, 091503 (2008).

[11] J. Abdallah *et al.* (DELPHI Collab.), Eur. Phys. J. **C45** 35 (2006).

[12] B. Aubert *et al.* (BABAR Collab.), Nucl. Instrum. Methods A **479**, 1 (2002).

[13] S. Agostinelli *et al.*, Nucl. Instrum. Methods A **506**, 250 (2003).

[14] D. Scora and N. Isgur, Phys. Rev. D **52**, 2783 (1995). See also N. Isgur *et al.*, Phys. Rev. D **39**, 799 (1989).

[15] J. L. Goity and W. Roberts, Phys. Rev. D **51**, 3459 (1995).

[16] B. Aubert *et al.* (BABAR Collab.), Phys. Rev. Lett. **92**, 071802 (2004).

[17] B. Aubert *et al.* (BABAR Collab.), Phys. Rev. D **69**, 111104 (2004).

[18] K. Cranmer, Comput. Phys. Commun. **136**, 198 (2001).

[19] V. Abazov *et al.* (DØ Collab.), Phys. Rev. Lett. **95**, 171803 (2005).